06-06 June 2006

TECH BRIEFS

NATIONAL AERONAUTICS AND SPACE ADMINISTRATION

INTRODUCTION

Tech Briefs are short announcements of innovations originating from research and development activities of the National Aeronautics and Space Administration. They emphasize information considered likely to be transferable across industrial, regional, or disciplinary lines and are issued to encourage commercial application.

Availability of NASA Tech Briefs and TSPs

Requests for individual Tech Briefs or for Technical Support Packages (TSPs) announced herein should be addressed to

National Technology Transfer Center

Telephone No. **(800) 678-6882** or via World Wide Web at **www2.nttc.edu/leads/**

Please reference the control numbers appearing at the end of each Tech Brief. Information on NASA's Innovative Partnerships Program (IPP), its documents, and services is also available at the same facility or on the World Wide Web at **http://ipp.nasa.gov**.

Innovative Partnerships Offices are located at NASA field centers to provide technology-transfer access to industrial users. Inquiries can be made by contacting NASA field centers and Mission Directorates listed below.

NASA Field Centers and Program Offices

Ames Research Center
Lisa L. Lockyer
(650) 604-1754
lisa.l.lockyer@nasa.gov

Dryden Flight Research Center
Gregory Poteat
(661) 276-3872
greg.poteat@dfrc.nasa.gov

Goddard Space Flight Center
Nona Cheeks
(301) 286-5810
Nona.K.Cheeks.1@nasa.gov

Jet Propulsion Laboratory
Ken Wolfenbarger
(818) 354-3821
james.k.wolfenbarger@jpl.nasa.gov

Johnson Space Center
Helen Lane
(713) 483-7165
helen.w.lane@nasa.gov

Kennedy Space Center
Jim Aliberti
(321) 867-6224
Jim.Aliberti-1@nasa.gov

Langley Research Center
Robert Yang
(757) 864-8020
robert.l.yang@nasa.gov

John H. Glenn Research Center at Lewis Field
Robert Lawrence
(216) 433-2921
robert.f.lawrence@nasa.gov

Marshall Space Flight Center
Vernotto McMillan
(256) 544-2615
vernotto.mcmillan@msfc.nasa.gov

Stennis Space Center
John Bailey
(228) 688-1660
john.w.bailey@nasa.gov

NASA Mission Directorates

At NASA Headquarters there are four Mission Directorates under which there are seven major program offices that develop and oversee technology projects of potential interest to industry:

Carl Ray
Small Business Innovation Research Program (SBIR) & Small Business Technology Transfer Program (STTR)
(202) 358-4652
carl.g.ray@nasa.gov

Merle Mckenzie
Innovative Partnerships Program (Code TD)
(202) 358-2560
merle.mckenzie@hq.nasa.gov

John Mankins
Exploration Systems Research and Technology Division
(202) 358-4659
john.c.mankins@nasa.gov

Terry Hertz
Aeronautics and Space Mission Directorate
(202) 358-4636
thertz@mail.hq.nasa.gov

Glen Mucklow
Mission and Systems Management Division (SMD)
(202) 358-2235
gmucklow@
mail.hq.nasa.gov

Granville Paules
Mission and Systems Management Division (SMD)
(202) 358-0706
gpaules@mtpe.hq.nasa.gov

Gene Trinh
Human Systems Research and Technology Division (ESMD)
(202) 358-1490
eugene.h.trinh@nasa.gov

John Rush
Space Communications Office (SOMD)
(202) 358-4819
john.j.rush@nasa.gov

TECH BRIEFS

NATIONAL AERONAUTICS AND SPACE ADMINISTRATION

Technology Focus: Test & Measurement

Magnetic-Field-Response Measurement-Acquisition System

Sensors are interrogated without physical connection to a power source, microprocessor, data-acquisition equipment, or electrical circuitry.

Langley Research Center, Hampton, Virginia

A measurement-acquisition system uses magnetic fields to power sensors and to acquire measurements from sensors. The system alleviates many shortcomings of traditional measurement-acquisition systems, which include a finite number of measurement channels, weight penalty associated with wires, use limited to a single type of measurement, wire degradation due to wear or chemical decay, and the logistics needed to add new sensors. Eliminating wiring for acquiring measurements can alleviate potential hazards associated with wires, such as damaged wires becoming ignition sources due to arcing.

The sensors are designed as electrically passive inductive-capacitive or passive inductive-capacitive-resistive circuits that produce magnetic-field re–sponses. One or more electrical parameters (inductance, capacitance, and resistance) of each sensor can be variable and corresponds to a measured physical state of interest. The magnetic-field-response attributes (frequency, amplitude, and bandwidth) of the inductor correspond to the states of physical properties for which each sensor measures.

For each sensor, the measurement-acquisition system produces a series of increasing magnetic-field harmonics within a frequency range dedicated to that sensor. For each harmonic, an antenna electrically coupled to an oscillating current (the frequency of which is that of the harmonic) produces an oscillating magnetic field. Faraday induction via the harmonic magnetic fields produces an electromotive force and therefore a current in the sensor. Once electrically active, the sensor produces its own harmonic magnetic field as the inductor stores and releases magnetic energy. The antenna of the measurement-acquisition system is switched from a transmitting to a receiving mode to acquire the magnetic-field response of the sensor. The rectified amplitude of the received response is compared to previous responses to prior transmitted harmonics, to ascertain if the measurement system has detected a response inflection. The "transmit-receive-compare" of sequential harmonics is repeated until the inflection is identified. The harmonic producing the amplitude inflection is the sensor resonant frequency. Resonant frequency and response amplitude are stored and then correlated to calibration data.

Multiple sensors can be interrogated using a single acquisition system. Each sensor must have a dedicated frequency partition of the antenna bandwidth, and the interrogation system must be augmented with a measurement correlation table for each sensor. The method eliminates the need for a data acquisition channel dedicated to each sensor. Any existing inductive or capacitive sensor can also be modified to be interrogated using this method.

The use of magnetic fields for powering sensors and for acquiring the measurements from them eliminates the need for physical connection from the sensors to a power source and data-acquisition equipment. Because magnetic fields are used to power the sensors that, in turn, respond with their own magnetic fields, the attributes of which are dependent upon the physical properties being measured, this class of sensors is referred to as magnetic-field-response sensors.

Figure 1. A **Portable Magnetic-Field-Response Recorder** is shown in a handheld version.

Because the functionality of the magnetic-field-response sensors is based upon magnetic fields, the sensors can be used under such conditions as in caustic environments, acids, high temperatures, cryogenic temperatures, high pressures, and radiative environments. Furthermore, the method allows acquiring measurements that were previously unattainable or logistically difficult because there was no practical means of getting power and data-acquisition electrical connections to a sensor. A novel feature of the method is that an individual sensor can be used to measure simultaneously more than one physical state. This is achieved by correlating combinations of different physical states to combinations of different sensor response attributes. Another novel feature of the method is that a sensor can be used to measure a permanent transition of one physical state to another. Once the new physical state has been achieved (e.g., material phase transition), the sensor can simultaneously measure other physical states.

The magnetic-field-response recorder shown in Figure 1 is a handheld version of the measurement-acquisition system using the method discussed. Figure 2 shows a fluid-level sensor being interrogated using the recorder internal antenna and an external antenna. The programmable recorder is designed to be simple to use and is capable of powering and acquiring measurements from any magnetic-field-response sensor. It can acquire and interpret measurements that correspond to either the amplitude, frequency, and/or bandwidth of the magnetic-field-response sensor. Resonant response frequency

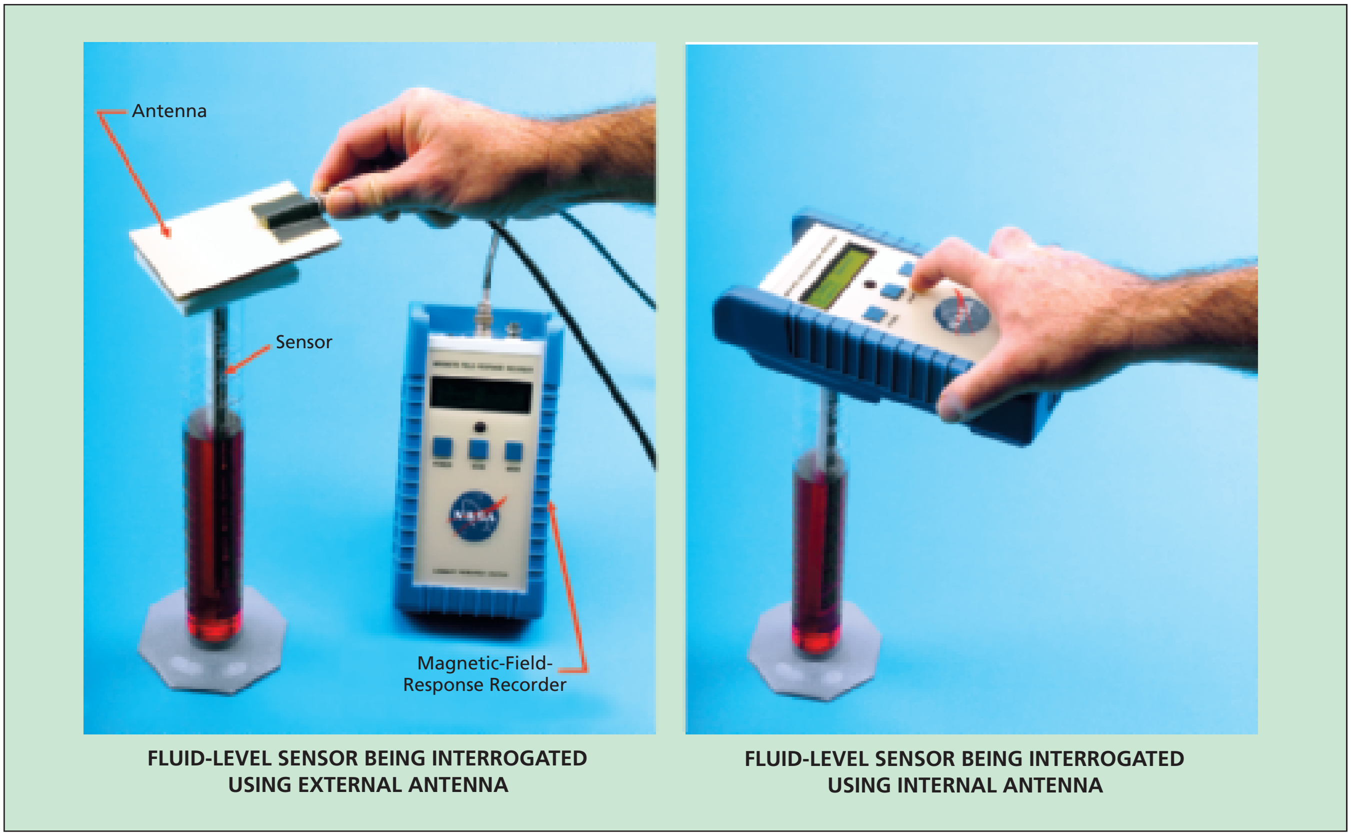

Figure 2. **Interrogation of a Wireless Fluid-Level Sensor** is shown using the magnetic-field-response recorder.

and amplitude of each sensor are displayed. The amplitude is dependent upon distance at which the sensor is interrogated. The recorder can be programmed to display the physical value of the measurement. The magnetic-field-response recorder has an internal antenna, connector for external antenna, and an analog output.

The measurement-acquisition method has many advantages over other methods currently in use. Once electrically excited, the sensors have very low voltage. If a short does occur in the sensor, the sensor will not be electrically active because a completed circuit is needed for Faraday induction. Hence, electrical arcing is prevented. Because the measurement system and sensors do not necessitate a physical connection to a power source or data-acquisition equipment, they are easy to implement into existing vehicles, structures, or other existing systems. The measurement system can be installed during any phase of vehicle life, and it is less costly to install new sensors than the traditional method of wiring a sensor to acquisition equipment. Such a system can be used to implement measurements that were not envisioned during design of a vehicle or structure but identified as needed during testing or operation. New measurements only require that the new sensors be placed within the magnetic field of the interrogating antenna(s). No wiring is required. Many of the sensors and interrogating antennas can be made lightweight and non-obtrusive by directly placing on the vehicle or structural components using metallic-film deposition methods.

This work was done by Stanley E. Woodard, Qamar A. Shams, and Robert L. Fox of **Langley Research Center** *and Virginia and Bryant D. Taylor of Swales Aerospace Corporation. Further information is contained in a TSP (see page 1).*
LAR-16908

Platform for Testing Robotic Vehicles on Simulated Terrain

Slope, ground material, and obstacles can be varied.

NASA's Jet Propulsion Laboratory, Pasadena, California

The variable terrain tilt platform (VTTP) is a means of providing simulated terrain for mobility testing of engineering models of the Mars Exploration Rovers. The VTTP could also be used for testing the ability of other robotic land vehicles (and small vehicles in general) to move across terrain under diverse conditions of slope and surface texture, and in the presence of obstacles of various sizes and shapes.

The VTTP consists mostly of a 16-ft-(4.88-m)-square tilt table. The tilt can be adjusted to any angle between 0° (horizontal) and 25°. The test surface of the table can be left bare; can be covered with hard, high-friction material; or can be covered with sand, gravel, and/or other ground-simulating material or combination of materials to a thickness of as much as 6 in. (≈15 cm).

A **Model Robotic Vehicle** was driven over 25-cm obstacles on simulated terrain at a tilt of 20°.

Models of rocks, trenches, and other obstacles can be placed on the simulated terrain.

For example, for one of the Mars-Rover tests, a high-friction mat was attached to the platform, then a 6-in.- (≈15 cm) deep layer of dry, loose beach sand was deposited on the mat. The choice of these two driving surface materials was meant to bound the range of variability of terrain that the rover was expected to encounter on the Martian surface. At each of the different angles at which tests were performed, for some of the tests, rocklike concrete obstacles ranging in height from 10 to 25 cm were placed in the path of the rover (see figure).

The development of the VTTP was accompanied by development of a methodology of testing to characterize the performance and modes of failure of a vehicle under test. In addition to variations in slope, ground material, and obstacles, testing typically includes driving up-slope, down-slope, cross-slope, and at intermediate angles relative to slope. Testing includes recording of drive-motor currents, wheel speeds, articulation of suspension mechanisms, and the actual path of the vehicle over the simulated terrain. The collected data can be used to compute curves that summarize torque, speed, power-demand, and slip characteristics of wheels during the traverse.

This work was done by Randel Lindemann of Caltech for **NASA's Jet Propulsion Laboratory**. *Further information is contained in a TSP (see page 1).*
NPO-42522

Interferometer for Low-Uncertainty Vector Metrology

Accuracy is increased; time and cost are reduced.

Goddard Space Flight Center, Greenbelt, Maryland

The figure is a simplified schematic diagram of a tilt-sensing unequal-path interferometer set up to measure the orientation of the normal vector of one surface of a cube mounted on a structure under test. This interferometer has been named a "theoferometer" to express both its interferometric nature and the intention to use it instead of an autocollimating theodolite.

The theoferometer optics are mounted on a plate, which is in turn mounted on orthogonal air bearings for near-360° rotation in azimuth and elevation. Rough alignment of the theoferometer to the test cube is done by hand, with fine position adjustment provided by a tangent arm drive using linear inchwormlike motors.

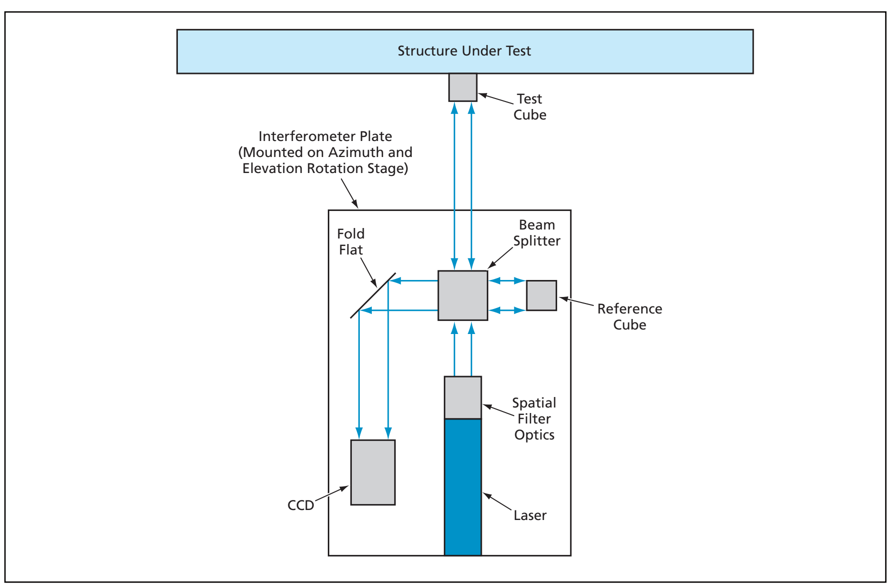

In this **Interferometer**, the interference pattern formed by the laser beams from the cubes is imaged onto the CCD. This pattern would depend on the angular misalignment between the cubes and would be analyzed to determine the misalignment.

In the operation of the theoferometer, the interference pattern formed by the collimated laser beams reflected from the two cubes is focused onto a charge-coupled device (CCD) detector. The resulting digitized interference fringe pattern is then analyzed by dedicated software to determine the angular misalignment between the two laser beams (and, hence, the misalignment between the cubes) at the sub-arcsecond level. If a null fringe pattern were achieved, it could be concluded that the laser beam points anti-parallel to the surface normal of the test cube. Knowledge of the distance from null (via the angular misalignment seen in the interference pattern) coupled with readings from azimuth and elevation encoders calibrated to the laser-pointing direction then gives the orientation of the cube surface normal vector in two (angular) dimensions. This is the same information as would be given by a theodolite aligned to the test cube, albeit with greater accuracy.

This system offers several advantages. The parts used in the prototype unit were off-the-shelf and relatively inexpensive. Whereas the uncertainty of a typical theodolite measurement is 1 to 2 arcseconds, the current theoferometer prototype has a demonstrated uncertainty of about 0.3 arcsecond. Moreover, the theoferometer makes it possible to completely automate the data-taking process, reducing the time required to take measurements. The net result is better metrology at lower cost, relative to metrology by use of an autocollimating theodolite.

This work was done by Ronald W. Toland and Douglas B. Leviton of **Goddard Space Flight Center**. *Further information is contained in a TSP (see page 1). GSC-14753-1*

Rayleigh Scattering for Measuring Flow in a Nozzle Testing Facility

The facility can test nozzles up to 8.75-in. (22.2-cm) in diameter.

John H. Glenn Research Center, Cleveland, Ohio

A molecular Rayleigh-scattering-based air-density measurement system was built in a large nozzle-and-engine-component test facility for surveying supersonic plumes from jet-engine exhaust. The facility (see Figure 1) can test nozzles up to 8.75 in. (22.2-cm) in diameter. It is enclosed in a 7.5-ft (2.3-m) diameter tank where ambient pressure is adjusted to simulate engine operation up to an altitude of 48,000 ft (14,630 m). The measurement technique depends on the light scattering by gas molecules present in the air; no artificial seeding is required. Commercially available particle-based techniques, such as laser Doppler velocimetry and particle image velocimetry, were avoided for such reasons as requirement of extremely large volume of seed particles; undesirable coating of every flow passages, model, and test windows with seed particles; and measurement errors from seed particles not following the flow. The molecular Rayleigh-scattering-based technique avoids all of these problems; however, a different set of obstacles associated with cleaning of dust particles, avoidance of stray light, and protection of the optical components from the facility vibration need to be addressed.

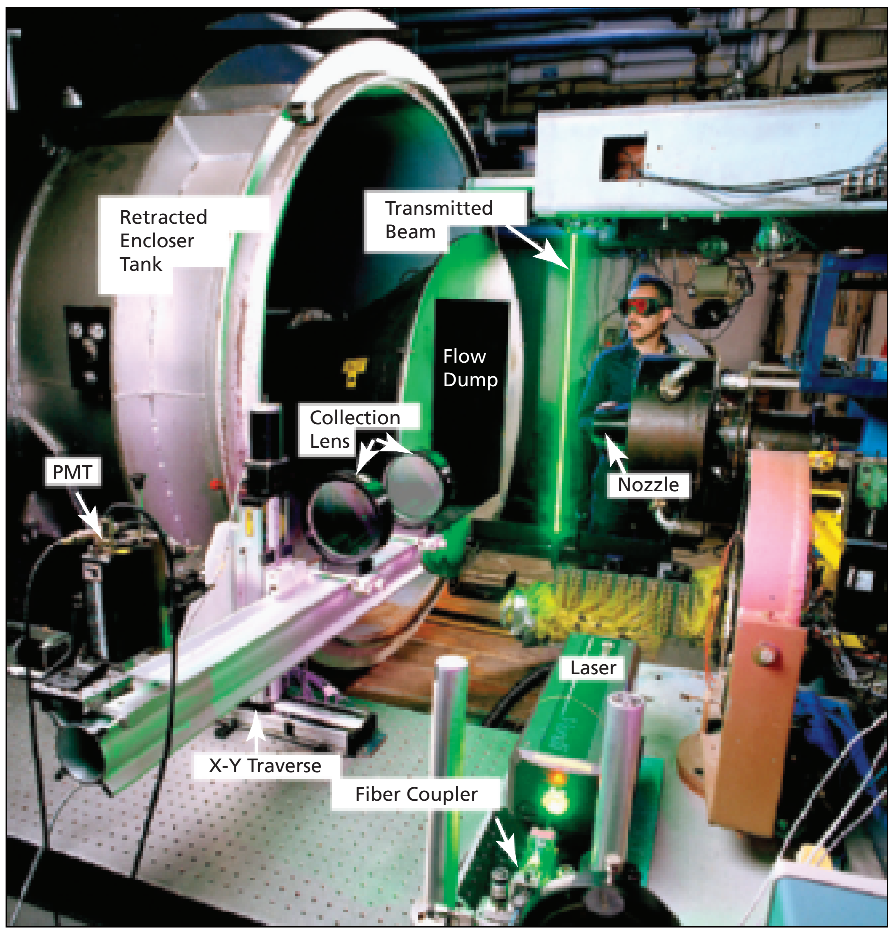

Fig. 1. The **Optical Arrangement** is shown with the enclosing tank retracted downstream.

To avoid a problem with facility vibration, light from a single-mode continuous-wave laser was transmitted into the vacuum tank by the use of an optical fiber. It was then collimated and passed through the plume. Rayleigh-scattered light from various points along the collimated beam was collected by a set of collection lenses placed outside the vacuum tank and measured by a photomultiplier tube (PMT). Large glass windows on the tank provided optical access. The collimator for the transmitted beam and the light-collection optics were placed on two synchronized traversing units to enable a survey over a cross-section of the nozzle plume. Although the technique is suitable to measure velocity, temperature, and density, in this

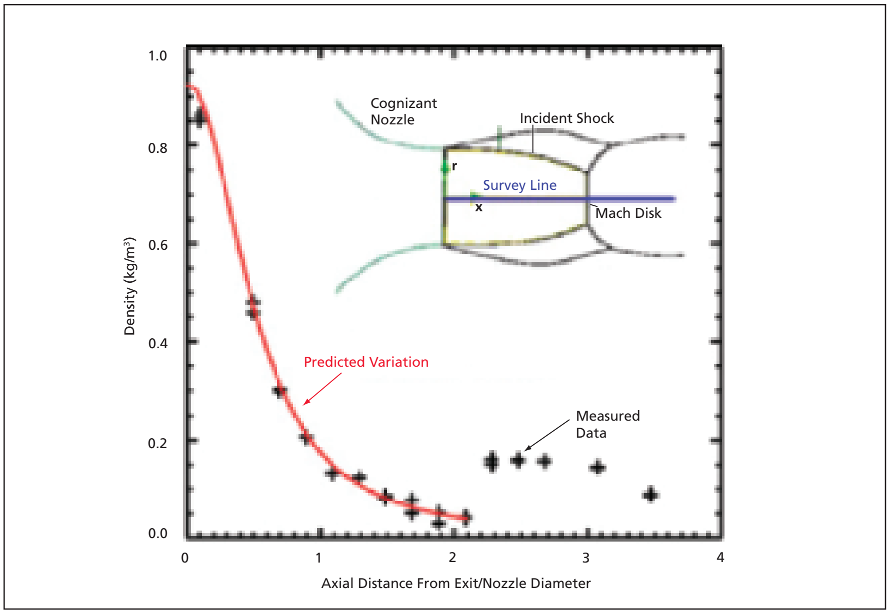

Fig. 2. **Density Variation** is shown along the centerline of a 5.06-in. (12.9-cm) diameter, nozzle-pressure-ratio 10, supersonic jet from a convergent nozzle.

first entry only air density was measured by monitoring intensity of the scattered light. Excellent comparison between theoretically predicted variation and the measured data along the centerline of a highly underexpanded supersonic jet provided validation to the measurement technique (see Figure 2).

This work was done by Carlos R. Gomez of **Glenn Research Center** *and Jayanta Panda of the Ohio Aerospace Institute. Further information is contained in a TSP (see page 1).*

Inquiries concerning rights for the commercial use of this invention should be addressed to:

NASA Glenn Research Center
Innovative Partnerships Office
Attn: Steve Fedor
Mail Stop 4–8
21000 Brookpark Road
Cleveland, Ohio 44135.

Refer to LEW-17627-1.

"Virtual Feel" Capaciflectors

Increases in capacitance with deviations from desired central positions would be exploited.

Goddard Space Flight Center, Greenbelt, Maryland

The term "virtual feel" denotes a type of capaciflector (an advanced capacitive proximity sensor) and a methodology for designing and using a sensor of this type to guide a robot in manipulating a tool (e.g., a wrench socket) into alignment with a mating fastener (e.g., a bolt head) or other electrically conductive object. Unlike robotic vision, capacitive proximity sensing does not require a clear line of sight to the mating fastener. On the contrary, capacitive proximity sensing affords the greatest position-measuring sensitivity in the situation in which it is most needed — when the tool is so close to the fastener as to prevent viewing.

Capaciflectors, other capacitive proximity sensors, and related developments have been described in numerous previous *NASA Tech Briefs* articles. Of those articles, the one most relevant to the present innovation was "Guiding Robots With The Help of Capaciflectors" (GSC-13614), *NASA Tech Briefs*, Vol. 21, No. 3 (March 1997), page 44. Like other capacitive proximity sensors, a capaciflector includes at least one sensing electrode, excited with an alternating voltage, that puts out a signal indicative of the capacitance between that electrode and a proximal object.

As described in the cited previous article, a robotic manipulator would be tipped with a tool instrumented with a capaciflector that would include an array of sensing electrodes that would be somewhat complex because it would be designed to enable three-dimensional proximity sensing. The outputs of the sensing electrodes would be converted to DC, digitized, then fed to a digital processor. In the processor, the variation of sensed capacitances with relative position and orientation of the capaciflector and a sensed object would be used to generate data equivalent to a fictitious force field that could be a source of signals to control the motion of the robotic manipulator in the vicinity of the object. Thus, collisions could be avoided and the manipulator could be guided into proximity and alignment with the intended object without making premature contact with the object. The initial approach would typically involve a raster scan of the manipulator while capaciflector outputs were processed to determine positions of closest approach in scan planes that were progressively brought closer to the object, without bringing them so close as to risk collision. This scan would yield data on the approximate position and orientation of the object relative to the manipulator. Following the scan, the capaciflector outputs would be processed and used for guidance as the manipulator was dithered into soft contact with the object.

The "virtual feel" capaciflector methodology also involves digitization and processing of capacitance readings as functions of relative position and orientation to obtain data equivalent to a fictitious force field that, in this case, is regarded as providing a quasi-tactile sense of imminent contact. However, a "virtual feel" capaciflector would be electronically and mechanically simpler because it would typically include only two electrodes: a sensing electrode and a shielding electrode. Moreover, the tool could serve as the sensing electrode. For example, if the tool were a wrench socket to be mated with a bolt head, then the wrench socket would be the sensing electrode (see figure). The sides of the wrench socket would be covered with a layer of electrically insulating material that would, in turn, be covered by a metallic outer shell that would serve as the shielding electrode. The capaciflector output would in-

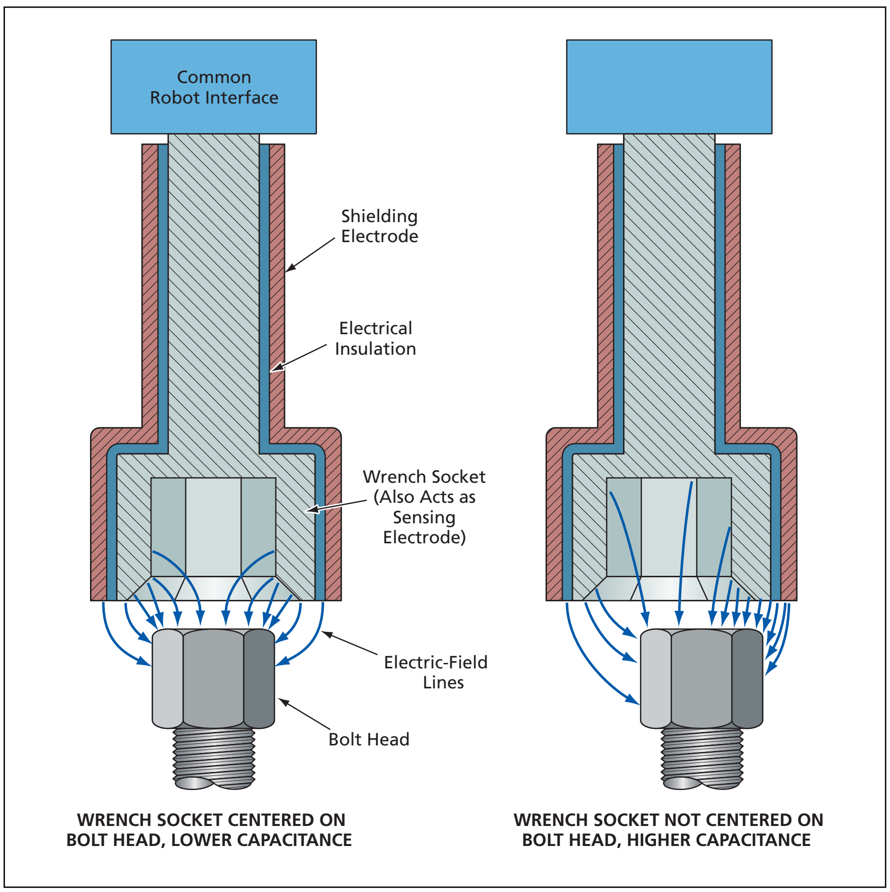

A **Wrench Socket** would double as the sensing electrode of a capaciflector. The capacitance between the bolt head and the wrench socket would be measured as the socket was dithered, in order to derive information needed to keep the socket centered on and clocked to the bolt head in preparation for mating.

dicate the capacitance between the wrench socket and the bolt head.

The algorithm processing the digitized capaciflector readings would exploit the fact that for any fixed position of the wrench socket along the central axis of the bolt head, the capacitance would reach a minimum when the axis of the wrench socket coincided with the axis of the bolt head and the wrench socket was clocked (rotated about its axis) to the angular position for mating with the bolt head: any lateral (horizontal in the figure) translation or any rotation of the wrench socket away from the central position and the mating orientation would cause an increase in capacitance. Hence, for a given fixed position along the center line of the bolt, the information needed to correct any deviation of the wrench socket from the central position and the mating orientation could be obtained by taking capacitance measurements during a sequence of controlled dithers of the position and orientation along and about the various coordinate axes. This is analogous to the feel a skilled craftsman instinctively uses, except it is noncontact, hence, "virtual feel."

This work was done by John M. Vranish of **Goddard Space Flight Center**. *Further information is contained in a TSP (see page 1).*

GSC-14955-1

FETs Based on Doped Polyaniline/Polyethylene Oxide Fibers

Advantages include tailorability of electronic properties and low power demands.

John H. Glenn Research Center, Cleveland, Ohio

A family of experimental highly miniaturized field-effect transistors (FETs) is based on exploitation of the electrical properties of nanofibers of polyaniline/polyethylene oxide (PANi/PEO) doped with camphorsulfonic acid. These polymer-based FETs have the potential for becoming building blocks of relatively inexpensive, low-voltage, high-speed logic circuits that could supplant complementary metal oxide/semiconductor (CMOS) logic circuits.

The development of these polymer-based FETs offers advantages over the competing development of FETs based on carbon nanotubes. Whereas it is difficult to control the molecular structures and, hence, the electrical properties of carbon nanotubes, it is easy to tailor the electrical properties of these polymer-based FETs, throughout the range from insulating through semiconducting to metallic, through choices of doping levels and chemical manipulation of polymer side chains. A further advantage of doped PANi/PEO nanofibers is that they can be made to draw very small currents and operate at low voltage levels, and thus are promising for applications in which there are requirements to use many FETs to obtain large computational capabilities while minimizing power demands.

Fabrication of an experimental FET in this family begins with the preparation of a substrate as follows: A layer of silicon dioxide between 50 and 200 nm thick is deposited on a highly doped (resistivity ≈0.01 Ω·cm) silicon substrate, then gold electrodes/contact stripes are deposited on the oxide. Next, one or more fibers of camphorsulphonic acid-doped PANi/PEO having diameters of the order of 100 nm are electrospun onto the substrate so as to span the gap between the gold electrodes (see Figure 1).

Figure 2 depicts measured current-versus-voltage characteristics of the device of Figure 1, showing that saturation channel currents occur at source-to-drain potentials that are surprisingly low, relative to those of CMOS FETs. The hole mobility in the depletion regime in this transistor was found to be 1.4×10^{-4} $cm^2/(V{\cdot}s)$, while the one-dimensional charge density at zero gate bias was esti-

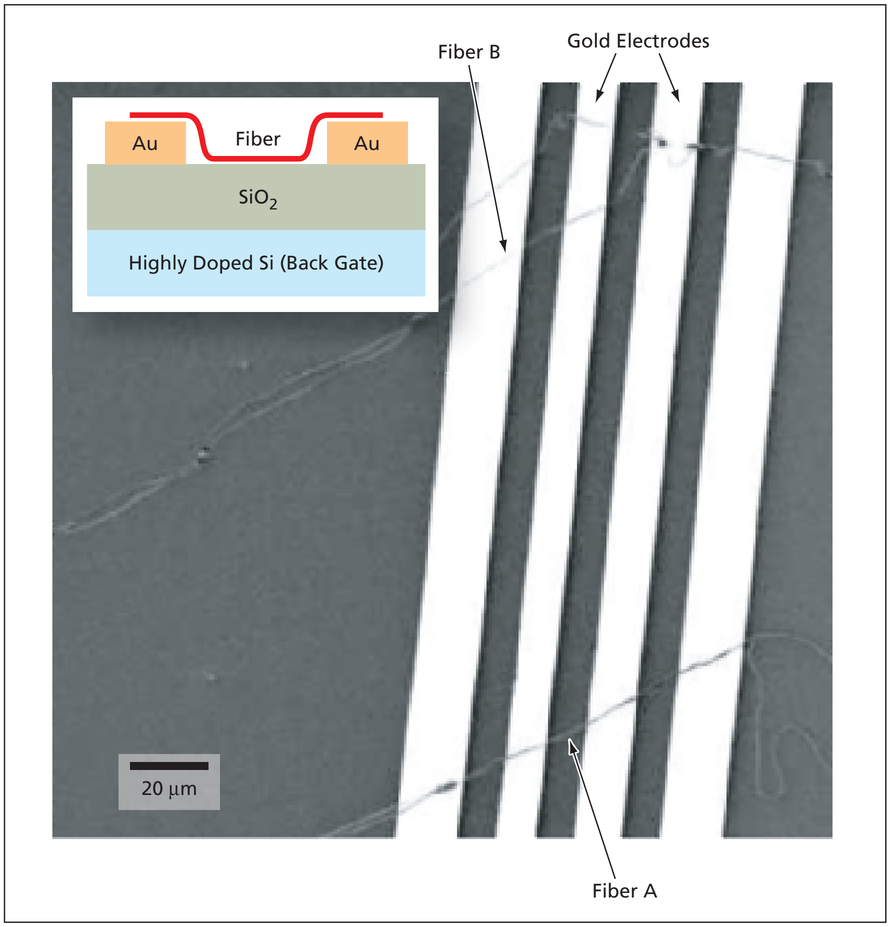

Figure 1. **Fibers of Doped PANi/PEO** are electrospun across the gap between source and drain gold electrodes on a prepared substrate to form an FET. The inset presents a simplified cross section showing one fiber. The rest of the picture is a scanning electron micrograph, wherein fiber A (12 µm long, 300 nm in diameter) and fiber B (18 µm long, 120 nm in diameter) in contact with the two inner gold electrodes are parts of an experimental FET.

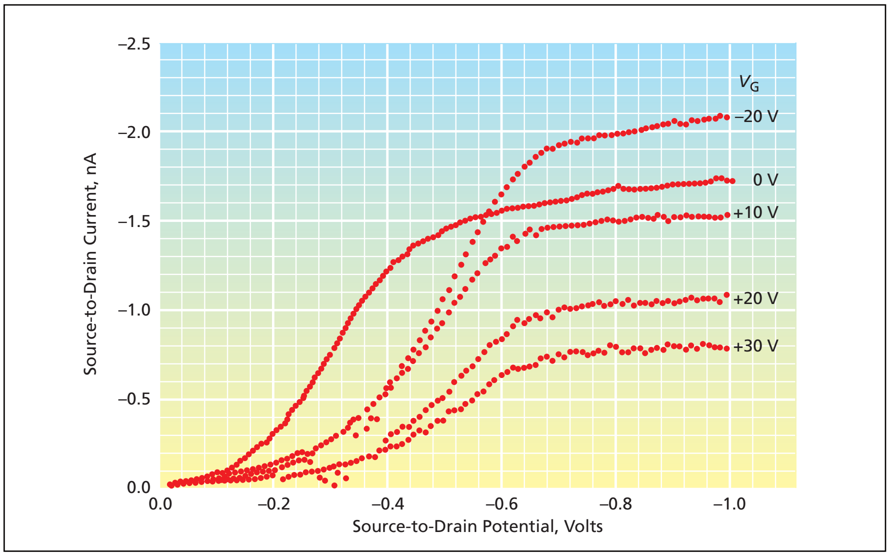

Figure 2. These **Current-Versus-Voltage Characteristics** were obtained from measurements on the FET of Figure 1. The measurements were made at various values of back gate voltage (VG) representative of the accumulation and depletion modes.

mated to be approximately one hole per 50 two-ring repeat units of polyaniline, consistent with the rather high channel conductivity (≈10^{-3} S/cm). Reducing or eliminating the PEO content of the fibers is expected to enhance the properties of future versions of this transistor.

This work was done by Noulie Theofylaktos, Daryl Robinson, and Félix Miranda of **Glenn Research Center***; Nicholas Pinto of the University of Puerto Rico; Alan Johnson, Jr. and Alan MacDiarmid of the University of Pennsylvania; and Carl Mueller of Analex Corp. Further information is contained in a TSP (see page 1).*

Inquiries concerning rights for the commercial use of this invention should be addressed to NASA Glenn Research Center, Innovative Partnerships Office, Attn: Steve Fedor, Mail Stop 4–8, 21000 Brookpark Road, Cleveland, Ohio 44135. Refer to LEW-17933-1.

Miniature Housings for Electronics With Standard Interfaces

Marshall Space Flight Center, Alabama

A family of general-purpose miniature housings has been designed to contain diverse sensors, actuators, and drive circuits plus associated digital electronic readout and control circuits. Each housing fits within an envelope having dimensions of about 2-¼ by 1-¾ by ½ in. (about 5.7 by 4.4 by 1.3 cm). Each housing can be secured to a mating carrier by use of screws or epoxy; this mounting scheme helps the housings and their contents to withstand severe vibrations and ensures thermal conduction for dissipation of heat generated during operation of the contained circuitry. The circuits contained in the housings communicate with the external world via standard RS-485 interfaces. Multiple units comprising housings and their contents can easily be electrically connected together in a daisy-chain arrangement, within which individual units are addressable via the RS-485 bus. Hence, a single master computer connected to the bus can program, or read data from, any or all such units. Examples of such units include small motor drives, programmable thermostats, data loggers, and programmable controllers. There are numerous potential uses for these units in medical equipment, automotive electronics, manufacturing equipment, and robots.

This work was done by David E. Howard, Dennis A. Smith, and Dean C. Alhorn of **Marshall Space Flight Center***. Further information is contained in a TSP (see page 1).*

This invention is owned by NASA, and a patent application has been filed. For further information, contact Sammy Nabors, MSFC Commercialization Assistance Lead, at sammy.a.nabors@nasa.gov. Refer to MFS-32000-1.

Software

Integrated Modeling Environment

The Integrated Modeling Environment (IME) is a software system that establishes a centralized Web-based interface for integrating people (who may be geographically dispersed), processes, and data involved in a common engineering project. The IME includes software tools for life-cycle management, configuration management, visualization, and collaboration. It enables organized, efficient communication of engineering analyses and the statuses thereof. Key functions performed by use of the IME include creation, further development, and management of modeling analyses over their entire life cycles; publishing model and analysis information for availability and reuse throughout the user community; and managing legacy information without regard to original formats, database organizations, or computing platforms. The use of the IME creates an archive of analysis results, plus documentation that identifies the assumptions and data elements used for each analysis. This archive is configured to enable reuse of previous analysis results, and tracing of types and versions of software used for each step of each analysis. The IME utilizes a customized version of a commercial product-life-cycle-management app-lication program that provides rich capabilities for managing configurations, workflows, data, and access through a single Web-based environment.

This program was written by Gary Mosier of **Goddard Space Flight Center**, *and Paul Stone and Christopher Holtery of Constellation Software Engineering Corp. Further information is contained in a TSP (see page 1).*
GSC-14827-1

Modified Recursive Hierarchical Segmentation of Data

An algorithm and a computer program that implements the algorithm that performs recursive hierarchical segmentation (RHSEG) of data have been developed. While the current implementation is for two-dimensional data having spatial characteristics (e.g., image, spectral, or spectral-image data), the generalized algorithm also applies to three-dimensional or higher dimensional data and also to data with no spatial characteristics. The algorithm and software are modified versions of a prior RHSEG algorithm and software, the outputs of which often contain processing-window artifacts including, for example, spurious segmentation-image regions along the boundaries of processing-window edges. The modification consists of the addition of an efficient subroutine through which pairs of regions are identified that may contain pixels that are actually more similar to other regions in the pair. Once these pairs of regions are identified, pixels in one region that are more similar to pixels in the other region are reassigned to the other region. The subroutine is computationally efficient because it focuses only on those regions that could potentially contribute to the processing-window artifacts. In addition, any adverse effect of the subroutine on the computational efficiency of the algorithm is minimized by executing the subroutine at a point in the algorithm such that switching of pixels between regions that are subsequently merged is avoided.

This program was written by James C. Tilton of **Goddard Space Flight Center**. *For further information, contact the Goddard Innovative Partnerships Office at (301) 286-5810. GSC-14681-1*

Sizing Structures and Predicting Weight of a Spacecraft

EZDESIT is a computer program for choosing the sizes of structural components and predicting the weight of a spacecraft, aircraft, or other vehicle. In designing a vehicle, EZDESIT is used in conjunction with a finite-element structural-analysis program: Each structural component is sized within EZDESIT to withstand the loads expected to be encountered during operation, then the weights of all the structural finite elements are added to obtain the structural weight of the vehicle. The sizing of the structural components elements also alters the stiffness properties of the finite-element model. The finite-element analysis and structural component sizing are iterated until the weight of the vehicle converges to a prescribed iterative difference. The results of the sizing can be reviewed in two ways:

1. An interactive session of the EZDESIT program enables review of the results in a table that shows component types, component weights, and failure modes; and
2. The results are read into a finite-element preprocessing-and-postprocessing program and displayed on a graphical representation of the model.

This program was written by Jeffrey Cerro and C. P. Shore of **Langley Research Center**. *Further information is contained in a TSP (see page 1).*
LAR-16878-1

Stress Testing of Data-Communication Networks

NetStress is a computer program that stress-tests a data-communication network and components thereof. NetStress comprises two components running, respectively, in a transmitting system and a receiving system connected to a network under test. The novelty of the program is that is has the capability to generate/receive varied network loading traffic profiles, which prior known programs were incapable of producing (i.e., various packet sizes and various packet rates all combined to make a pseudo-random traffic pattern). The transmitting-system component generates increasingly stressful data traffic for transmission via the network. The receiving-system component analyzes the resulting traffic arriving in the receiving system, generating such statistics as the number of data packets successfully received, the number of dropped packets, and the number of packets received out of order. The packet sizes must be configured before the transmitting-system component is started, but the packet frequencies, numbers of packets in bursts, and burst times can be configured during execution. Typically, a test begins with transmission of data at low sustained rates. Then the sustained rates are increased and burst rates are modified while monitoring to determine whether the receiving-system component reports any losses. When significant losses are reported, the user seeks to determine whether a malfunction or deficiency has been found or normal network saturation has been attained. NetStress was written for execution in the VxWorks real-time operating system, but could easily be ported to other operating systems.

This program was written by Kurt Leucht and Guy Bedette of **Kennedy Space Center**. *For further information, contact the Kennedy Innovative Partnerships Office at (321) 861-7158.*
KSC-12589

Framework for Flexible Security in Group Communications

The Antigone software system defines a framework for the flexible definition and implementation of security policies in group communication systems. Antigone does not dictate the available security policies, but provides high-level mechanisms for implementing them. A central element of the Antigone architecture is a suite of such mechanisms comprising micro-protocols that provide the basic services needed by secure groups. Policies are implemented through the composition and configuration of these mechanisms. Mechanisms are composed in different ways to address new requirements and environmental constraints. The Antigone framework provides an easy-to-use application programming interface (API), from which secure group application programs can be built. Written entirely in the C++ programming language, the system consists of over 18,000 lines of source code and has been ported to several versions of Linux, FreeBSD, and SunOS. Information for accessing recent versions of the source code and related documentation is available at http://antigone.eecs.umich.edu.

This program was written by Patrick McDaniel and Atul Prakash of the University of Michigan for **Kennedy Space Center**.

In accordance with Public Law 96-517, the contractor has elected to retain title to this invention. Inquiries concerning rights for its commercial use should be addressed to:

Electrical Engineering and
Computer Sciences Department
University of Michigan
3115 EECS
1301 Beal Ave.
Ann Arbor, MI 48109

Refer to KSC-12207, volume and number of this NASA Tech Briefs *issue, and the page number.*

Software for Collaborative Use of Large Interactive Displays

The MERBoard Collaborative Workspace, which is currently being deployed to support the Mars Exploration Rover (MER) Missions, is the first instantiation of a new computing architecture designed to support collaborative and group computing using computing devices situated in NASA mission operations rooms. It is a software system for generation of large-screen interactive displays by multiple users. The architecture provides a platform and applications programming interface (API) for the development of collaborative applications for NASA mission operations. The standard deployment configuration provides an integrated whiteboard, Web browser, remote viewing and control for collaboration over distance, and personal and group storage spaces that provide ubiquitous access and sharing of data. Customization for specific domains is provided through plug-ins. For the MER mission, plug-ins include a flowcharting tool for strategic rover operations and mission planning, 3D visualization of the Martian terrain, a data navigator to navigate the mission database, and situational awareness tools. The MERBoard software is designed to run on large plasma displays with touchscreen overlays, thus providing an immersive and interactive environment for teams to view, annotate, and share data. The MERBoard overcomes the obstacles to communication, retention, and collaborative modification of information in diverse forms that can include text, data (including images) from scientific instruments, handwritten notes, hand drawings, and computer graphics. The MERBoard provides a unifying interface for the integration of heterogeneous applications, and provides those applications with a consistent model for saving and retrieving data. All applications may be viewed and controlled from any location that has a MERBoard. A personal client provides integration of a user's personal computing environment with the MERBoard environment.

This program was written by Jay Trimble, Thodore Shab, Roxana Wales, Alonso Vera, Irene Tollinger, Michael McCurdy, and Dmitriy Lyubimov at **Ames Research Center**. *For further information, contact the Ames Technology Partnerships Division at (650) 604-2954.*
ARC-14951-1

Materials

Microsphere Insulation Panels

Thermal performance and lifetime exceed those of foam insulation.

John F. Kennedy Space Center, Florida

Microsphere insulation panels (MIPs) have been developed as lightweight, long-lasting replacements for the foam and vacuum-jacketed systems heretofore used for thermally insulating cryogenic vessels and transfer ducts. Whether preformed or applied in place, foam insulation deteriorates fairly rapidly: on cryogenic transfer lines, it has a life expectancy of about three years. Vacuum-jacketed insulation is expensive and heavy. For both foam and vacuum-jacketed insulation, intensive maintenance is necessary to keep performance at or near its original level. Relative to a polyurethane foam insulation panel, a comparable MIP offers greater thermal performance and longer service life at approximately the same initial cost.

The microsphere core material of a typical MIP consists of hollow glass bubbles, which have a combination of advantageous mechanical, chemical, and thermal-insulation properties heretofore available only separately in different materials. In particular, a core filling of glass microspheres has high crush strength and low density, is noncombustible, and performs well in soft vacuum. A typical MIP includes microspheres in an evacuated space between flexible vacuum-barrier layers made of a multilayer polyester-based laminate [Mylar® 250SBL300 (or equivalent)]. Included in the laminate are several non-foil layers that serve as barriers to permeation by water vapor and other atmospheric gases. The polyester-based laminate material has a projected life in excess of 20 years.

An MIP can be made in clamshell-like halves that can be fitted into a cryogenic vessel or transfer duct. In general, MIPs can be applied to transfer ducts along with jacketing materials conventionally used on foam insulation, and can be installed by use of essentially the same techniques used to install preformed foam insulation. On the basis of tests according to standards C518 and C177 of the American Society for Testing and Materials, the thermal performance of a flexible vacuum-barrier MIP is about two times better than that of a comparable polyurethane foam insulation panel.

This work was done by R. Mohling, M. Allen, and R. Baumgartner of Technology Applications, Inc. for **Kennedy Space Center**. *For further information, contact Rolf Baumgartner at (303) 443-2262 x115 or rbaumga@techapps.com.*

In accordance with Public Law 96-517, the contractor has elected to retain title to this invention. Inquiries concerning rights for its commercial use should be addressed to:

Technology Applications, Inc.
5700 Flatiron Parkway, #5701A
Boulder, CO 80301-5733

Refer to KSC-12675, volume and number of this NASA Tech Briefs *issue, and the page number.*

Single-Wall Carbon Nanotube Anodes for Lithium Cells

Capacities are greater than those of graphite anodes.

John H. Glenn Research Center, Cleveland, Ohio

In recent experiments, highly purified batches of single-wall carbon nanotubes (SWCNTs) have shown promise as superior alternatives to the graphitic carbon-black anode materials heretofore used in rechargeable thin-film lithium power cells. The basic idea underlying the experiments is that relative to a given mass of graphitic carbon-black anode material, an equal mass of SWCNTs can be expected to have greater lithium-storage and charge/discharge capacities. The reason for this expectation is that whereas the microstructure and nanostructure of a graphitic carbon black is such as to make most of the interior of the material inaccessible for intercalation of lithium, a batch of SWCNTs can be made to have a much more open microstructure and nanostructure, such

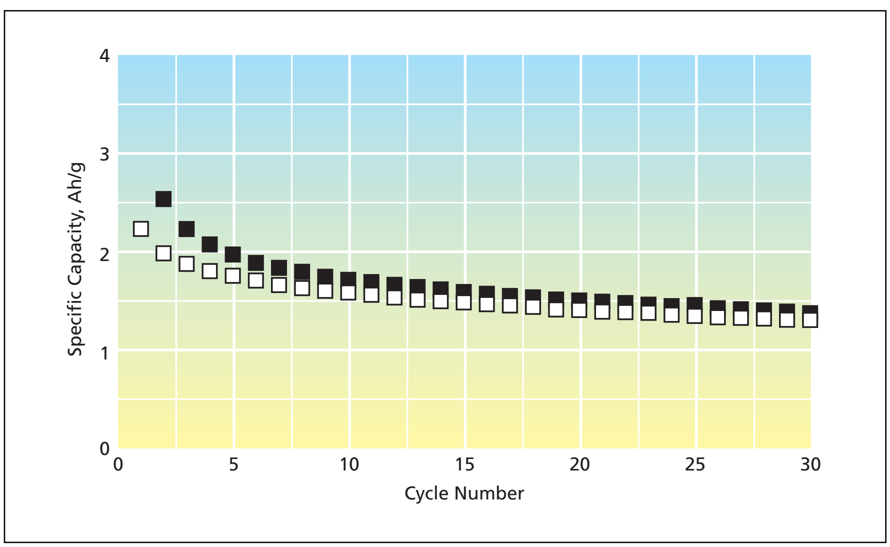

Specific Capacity of a carbon-nanotube anode material as a function of cycle number was calculated from charge and discharge times measured in galvanostatic cycling.

that most of the interior of the material is accessible for intercalation of lithium. Moreover, the greater accessibility of SWCNT structures can be expected to translate to greater mobilities for ion-exchange processes and, hence, an ability to sustain greater charge and discharge current densities.

For the experiments, soot containing carbon nanotubes was produced by laser vaporization of a graphite target containing 1.2 atomic percent Ni/Co in an argon atmosphere at a pressure of 500 torr (≈ 67 kPa) at a temperature of 1,200 °C. The soot was purified by refluxing in nitric acid at a temperature of 125 °C followed by annealing in oxygen at 550 °C for 30 minutes. By means of scanning electron microscopy, transmission electron microscopy, ultraviolet-visible spectrophotometry, and thermogravimetric analysis, 99 weight percent of the purified soot was found to consist of SWCNTs. The specific surface area of the purified material, as measured by use of the Brunauer, Emmett, and Teller (BET) technique based on adsorption of nitrogen, was found to be 1,200 m^2/g — much greater than the specific surface areas of several other carbonaceous anode materials that were also subjected to the BET test.

Anodes were fabricated by casting, onto copper foils, thin films of the purified SWCNT material dispersed at a concentration of 5 weight percent in poly(vinylidiene fluoride). The anodes were incorporated into standard three-electrode test cells along with lithium-foil counter and reference electrodes and an electrolyte comprising 1.0 M $LiPF_6$ in a solution of ethylene carbonate (2 parts by volume) and dimethyl carbonate (1 part by volume). Over-potentials for interaction of the anodes with lithium and lithium capacities of the anodes were measured by use of cyclic voltammetry and galvanostatic cycling, respectively.

The figure shows representative charge and discharge capacities determined from the measurements. The plotted values show a high degree of reversibility after the initial cycle. The specific capacity after 30 cycles was found to be about 1.33 Ah/g — almost 3 times the generally accepted value (0.45 Ah/g) for graphite.

This work was done by Aloysius F. Hepp of **Glenn Research Center***; Ryne Raffaelle and Tom Gennett of Rochester Institute of Technology; Prashant Kumta and Jeff Maranchi of Carnegie-Mellon University; and Mike Heben of National Renewable Energy Laboratory. Further information is contained in a TSP (see page 1).*

Inquiries concerning rights for the commercial use of this invention should be addressed to NASA Glenn Research Center, Commercial Technology Office, Attn: Steve Fedor, Mail Stop 4–8, 21000 Brookpark Road, Cleveland, Ohio 44135. Refer to LEW-17356-1

Tantalum-Based Ceramics for Refractory Composites

Compositions can be graded from porous substrates to impervious outer layers.

Ames Research Center, Moffett Field, California

A family of tantalum-based ceramics has been invented as ingredients of high-temperature composite insulating tiles. These materials are suitable for coating and/or permeating the outer layers of rigid porous (foamlike or fibrous) ceramic substrates to (1) render the resulting composite ceramic tiles impervious to hot gases and (2) enable the tiles to survive high heat fluxes at temperatures that can exceed 3,000 °F (≈1,600 °C). Originally intended for use on the future space exploration vehicles, insulating tiles made with these materials may also be useful in terrestrial applications (e.g., some industrial processes) in which there are requirements to protect against flows of hot, oxidizing gases.

The starting ingredients of a ceramic of this invention are the following:

- Tantalum disilicide ($TaSi_2$), which can act as either an emittance agent or a matrix material, depending upon the overall composition;
- Molybdenum disilicide ($MoSi_2$), which, depending on the overall composition, acts as a secondary emittance agent or as an oxygen getter (to inhibit the oxidation of tantalum within the finished composite);
- A borosilicate glass ($B_2O_3 \cdot SiO_2$), which acts as a source of boron and may, depending on the overall composition, act as an alternative matrix; and
- Silicon hexaboride (SiB_6), which acts as a processing aid by facilitating sintering of the aforementioned ingredients.

These ingredients are milled together in ethanol, and the resulting slurry is sprayed or painted onto a porous ceramic substrate. The underlying layers (sub-layers) of different compositions are used to integrate the outer layer (coating) with a wide variety of porous substrate materials. For this purpose, infiltration of these compositions into the substrate results in a functional gradient system that accounts for the difference in the coefficient of thermal expansion (CTE) between coating and substrate. The preferred composition for such underlying layers are in the approximate range of 20 to 60 weight percent of $MoSi_2$, 0 to 60 weight percent of $TaSi_2$, 40 to 80 weight percent of borosilicate glass, and 1 to 5 percent of SiB_6. The ingredients are then sintered by heating the treated substrate at atmospheric pressure at either a temperature of 2,225 °F (≈1,218 °C) for 90 minutes or a temperature of 2,400 °F (≈1,316 °C) for 10 minutes. The milling, coating, and sintering process conditions are chosen to minimize the undesired oxidation of tantalum compounds.

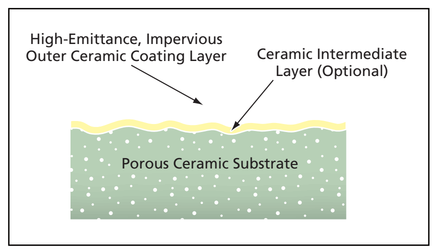

A **Porous Ceramic Substrate Is Coated** with one or more ceramic layers to render it impervious to hot gas and increase its ability to withstand high heat flux.

For an outer coating layer, the preferred composition is between 20 and 45 weight percent of borosilicate glass, between 10 and 65 weight percent of $TaSi_2$, between 5 and 30 weight percent of $MoSi_2$, and between 1 and 5 weight percent of SiB_6. An underlying layer or sublayer of different composition can be used to integrate the outer layer with the substrate and, for this purpose, may be allowed to infiltrate to some small depth below the surface of the substrate. The preferred composition for such an underlying layer lies in the approximate range of 20 to 60 weight percent of

$MoSi_2$, 40 to 80 weight percent of $B_2O_3 \cdot SiO_2$, and 1 to 5 percent of SiB_6. One or more intervening layer(s) of intermediate composition(s) could also be included (see figure). The precise composition of the sublayer should be chosen to match the CTE of the substrate, while the compositions of intermediate layers should be chosen to grade the transition from the CTE and porosity of the substrate to the CTE and full density of the outer coating layer.

This work was done by David A. Stewart, Daniel Leiser, Robert DiFiore, and Victor Katvala of **Ames Research Center**.

This invention is owned by NASA, and a patent application has been filed. Inquiries concerning rights for the commercial use of this invention should be addressed to the Ames Technology Partnerships Division at (650) 604-2954. Refer to ARC-14743-1.

Integral Flexure Mounts for Metal Mirrors for Cryogenic Use

These mounts are compact and relatively inexpensive.

Goddard Space Flight Center, Greenbelt, Maryland

Semi-kinematic, six-degree-of-freedom flexure mounts have been incorporated as integral parts of metal mirrors designed to be used under cryogenic conditions as parts of an astronomical instrument. The design of the mirrors and their integral flexure mounts can also be adapted to other instruments and other operating temperatures. In comparison with prior kinematic cryogenic mirror mounts, the present mounts are more compact and can be fabricated easily using Ram-EDM (electrical discharge machining) process.

The mirrors are designed to be mounted on an optical bench. To prevent bimetallic stresses that would arise during heating and cooling between room temperature (≈293 K) and the operating temperature of 80 K, both the optical bench and the mirrors are made of aluminum alloy 6061. Also, the mirrors and the bench are subjected to stress-relief treatments during fabrication to reduce figure errors and alignment changes that could arise upon cooling from room temperature to the operating temperature.

Each mirror has a width-to-thickness ratio of about 6 and is made from a 6061 aluminum alloy substrate. Three tablike flexures (mounting tabs) are machined into the rear of the substrate, which is diamond-machined flat to optical tolerances. The mounting tabs flex in six degrees of freedom, minimizing distortion caused by mounting the mirror on the bench. A large, thin, one-piece shim is placed between the rear surface of the mirror and the bench. The bench interface surface and the bench side of the shim are lapped flat for smooth, repeatable placement. Three thin, raised bosses that are flat and coplanar to within tight tolerances rise from the mirror side of the shim to meet the tabs. For changes in alignment, the bosses are machined such that the mirror substrate is always approximately parallel to the plane that the bosses define. Therefore, the tabs do not bend in response to changes in alignment, but flex only to accommodate coplanarity errors in the machining of the three shim bosses. Ideally, no tab should ever be made to flex more than ±0.025 mm in translation, but the tabs are designed to yield an acceptable figure error for displacements of as much as ±0.125 mm in all three translational degrees of freedom and/or ±0.1° in all three rotational degrees of freedom.

This work was done by S. Wahid Zewari, Jason E. Hylan, Sandra M. Irish, and Raymond G. Ohl of **Goddard Space Flight Center** *and Shelly B. Conkey of Swales Aerospace, Inc. Further information is contained in a TSP (see page 1).*
GSC-14969-1

Manufacturing & Prototyping

Templates for Fabricating Nanowire/Nanoconduit-Based Devices

Prior templating processes are being extended to finer spatial resolutions.

NASA's Jet Propulsion Laboratory, Pasadena, California

An effort is underway to develop processes for making templates that could be used as deposition molds and etching masks in the fabrication of devices containing arrays of nanowires and/or nanoconduits. Examples of such devices include thermoelectric devices, nerve guidance scaffolds for nerve repair, photonic-band-gap devices, filters for trapping microscopic particles suspended in liquids, microfluidic devices, and size-selective chemical sensors. The technology is an extension of previous work conducted by JPL, UCSD (University of California, San Diego), and Paradigm Optics Inc., which developed a process to fabricate macroporous scaffolds for spinal-cord repair.

Highly-ordered, optical-fiber arrays consisting of dissimilar polymers comprise the template technology. The selective removal of the fiber cores in specific solvents creates the porous templates to be filled with a "top-down" deposition process such as electrochemical deposition, sputter deposition, molecular beam epitaxy, and the like.

Typically, the fiber bundles consist of polystyrene (PS) fiber cores, which are clad with varying thickness poly(methyl methacrylate) (PMMA). When arranged in hexagonal, close-packed configuration and pulled, the fibers form highly-ordered arrays comprised of PS fiber cores surrounded by a continuous matrix of PMMA. The ratio of PMMA cladding thickness to PS core diameter determines the spacing between PS fiber cores and typically ranges from 3:1 to 1:1.

Essentially, the simultaneous heating and drawing or pulling in the longitudinal direction of polymer-fiber arrays fuses the fibers to-gether. Since the fusing process is a constant volume process, a lateral or cross-section reduction is accompanied by a commensurate increase in length. Thus, the degree of pulling determines the final core dimensions.

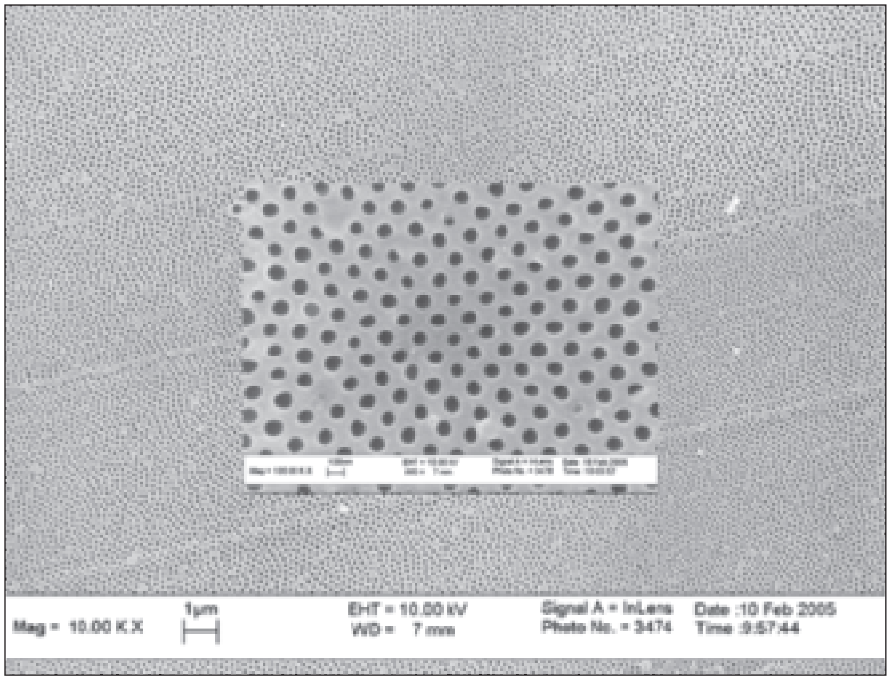

Figure 1. An **Image** from a scanning electron microscope shows the array of 100-nm diameter holes etched in a PMMA matrix.

Compared to previous work, where the fiber cores were in the range of 100 to 200 microns, the extent of pulling was significantly increased, thus resulting in a significant reduction in feature dimensions. The scanning electron microscope (Figure 1) image reveals the close packed array 100-nm diameter holes etched in a PMMA matrix (center image). The background image indicates that the hole monodispersity and order is maintained over relatively large areas. The original template length or fiber length was greater than 1 cm and the cross sectional dimension was 1 cm by 0.4 cm (Figure 2). In principle, the depth of the holes could be far greater than 1 mm, which could result in

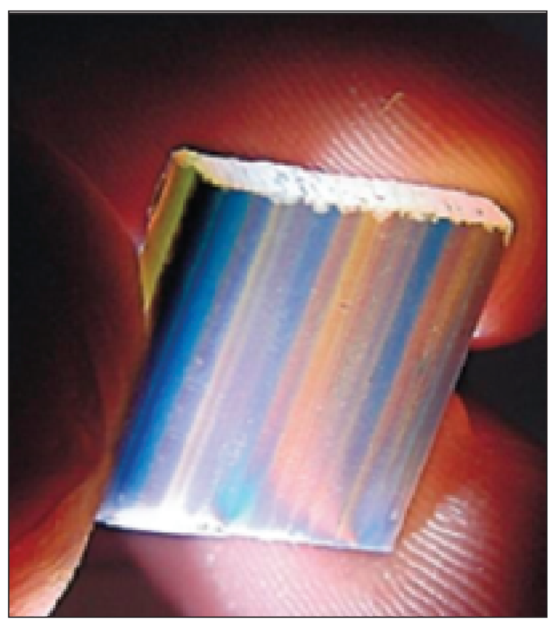

Figure 2. The **Nanotemplate**, approximately 1/2×1/2×1/8 inch (12.7×12.7×3.2 mm), contains about 60 fibers.

features with aspect ratios (length/diameter) in the 1,000 to 10,000 range.

This work was done by Jeffrey Sakamoto of Caltech for **NASA's Jet Propulsion Laboratory**, *and Todd Holt and David Welker of Paradigm Optics, Inc. Further information is contained in a TSP (see page 1).*

In accordance with Public Law 96-517, the contractor has elected to retain title to this invention. Inquiries concerning rights for its commercial use should be addressed to:

Innovative Technology Assets Management
JPL
Mail Stop 202-233
4800 Oak Grove Drive
Pasadena, CA 91109-8099
(818) 354-2240

Refer to NPO-41906, volume and number of this NASA Tech Briefs *issue, and the page number.*

Measuring Vapors To Monitor the State of Cure of a Resin

Excess curing time would no longer be needed as margin against uncertainty.

Langley Research Center, Hampton, Virginia

A proposed noninvasive method of monitoring the cure path and the state of cure of an epoxy or other resin involves measurement of the concentration(s) of one or more compound(s) in the vaporous effluent emitted during the curing process. The method is based on the following general ideas:

- The concentrations of the effluent compounds in the vicinity of the curing resin are approximately proportional to the instantaneous rate of curing.
- As curing proceeds at a given temperature, subsequent decreases in the concentrations are indicative of approaching completion of cure; that is, the lower are the concentrations, the more nearly complete is the cure.

The method could be utilized as the basis of a means of controlling the curing process to optimize the properties of the cured resin. It also could be utilized to minimize the cost of the curing process by ensuring a complete cure without the need to provide for excess curing time as margin against uncertainty in a prior estimate of required curing time.

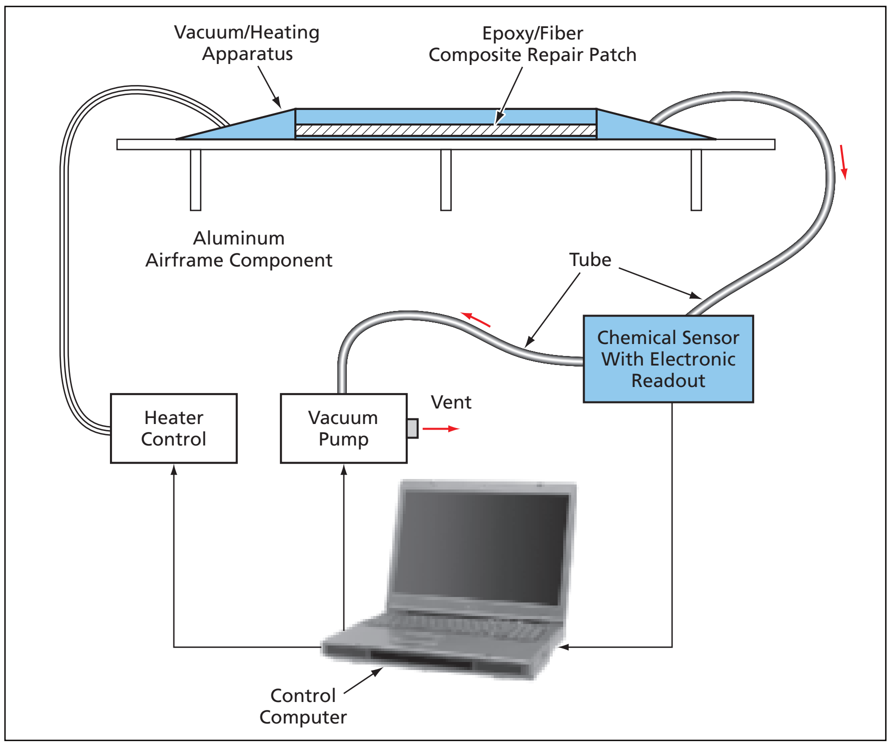

Curing of Epoxy in a composite patch on an aluminum airframe component would be monitored by measuring concentrations of vaporous effluent compounds. The measurements could serve as feedback for controlling the vacuum pump and the heater.

A system to implement the method would include a sensor that produces electronic readouts of the concentrations of effluent compounds of interest. This sensor could be any of a variety of instruments, ranging from general-purpose full-size laboratory instruments capable of rapidly analyzing many compounds to microelectromechanical (MEMS) devices designed to detect effluent compounds specific to one epoxy. Either continuously or at regular intervals, the sensor would sample the effluent. Depending on the specific curing process, the sampling could occur at room temperature, at elevated temperature, under vacuum, or at atmospheric pressure: for example, in a case involving curing in a vacuum/heating apparatus, the sensor could be placed in the unheated tube from the vacuum bag to the vacuum pump.

The concentration(s) of the compound(s) of interest, and, thus, the rate of production of effluent would be monitored electronically and digitized to make a record of the curing process. Once the concentrations of the effluent compounds of interest decreased to predetermined levels, the cure would be considered complete and the operator would be so notified by the sensor circuitry. Alternatively, as depicted schematically in the figure, the sensor could be integrated into a control loop that would turn off the curing apparatus upon completion of the cure. Further, the control loop could be configured for active control to maintain the rate of curing at a predetermined level by monitoring the effluent-production rate and automatically adjusting the temperature and/or the pressure of the partial vacuum.

This work was done by K. Elliott Cramer, Daniel F. Perey, and William T. Yost of **Langley Research Center**. *Further information is contained in a TSP (see page 1).*
LAR-16695-1

Physical Sciences

Partial-Vacuum-Gasketed Electrochemical Corrosion Cell

This cell is designed to reduce the incidence of crevice corrosion.

John F. Kennedy Space Center, Florida

An electrochemical cell for making corrosion measurements has been designed to prevent or reduce crevice corrosion, which is a common source of error in prior such cells. In a typical prior corrosion cell, crevice corrosion occurs at an interface between a material specimen, an electrolyte, and a specimen-mounting fixture. Crevice corrosion significantly alters current and voltage responses, thereby generating errors in the determination of both the thermodynamic and kinetic aspects of corrosion.

The present cell (see figure) includes an electrolyte reservoir with O-ring-edged opening at the bottom. In preparation for a test, the reservoir, while empty, is pressed down against a horizontal specimen surface to form an O-ring seal. A purge of air or other suitable gas is begun in the reservoir, and the pressure in the reservoir is regulated to maintain a partial vacuum. While maintaining the purge and partial vacuum, and without opening the interior of the reservoir to the atmosphere, the electrolyte is pumped into the reservoir. The reservoir is then slowly lifted a short distance off the specimen. The level of the partial vacuum is chosen such that the differential pressure is just sufficient to keep the electrolyte from flowing out of the reservoir through the small O-ring/specimen gap. Electrochemical measurements are then made. Because there is no gasket (and, hence, no crevice between the specimen and the gasket), crevice corrosion is unlikely to occur.

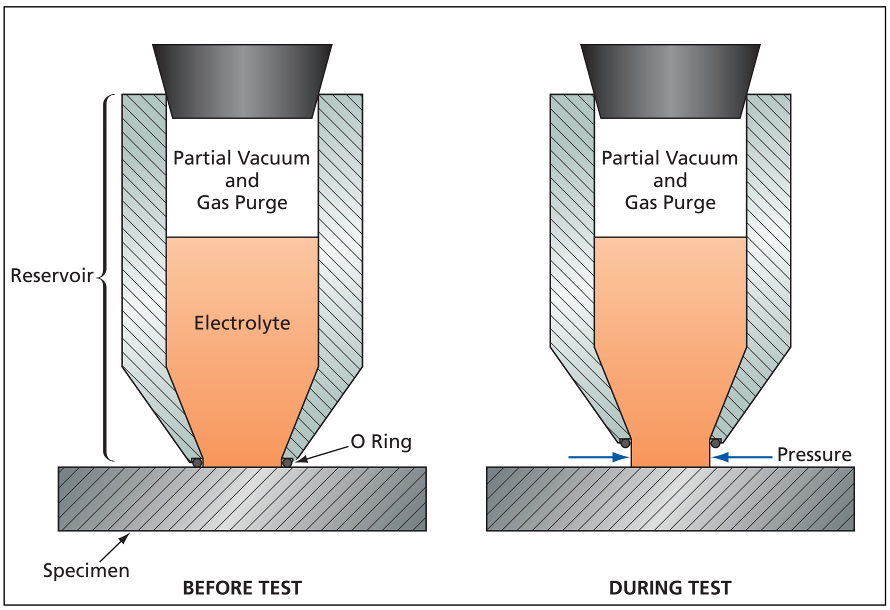

Differential Pressure between the atmosphere and the partial vacuum above the reservoir keeps the electrolyte in the reservoir when the reservoir is lifted a short distance off the specimen. The gap between the bottom of the reservoir and the specimen is exaggerated here for clarity.

This cell is easy to operate, uses a relatively small volume (10 to 25 mL) of electrolyte, accommodates specimens of various sizes, does not leave rubber O-ring residues on specimens, is inherently suitable for testing with electrolytes that must be purged with gases, and can easily be cleaned. Simple modifications can be performed to enable use of this cell in special crevice-free corrosion tests — for example, tests for determining critical pitting temperatures.

Inasmuch as the purge gas can quickly diffuse into the electrolyte, careful selection of the purge gas is necessary to ensure reliable results. Water-line corrosion could introduce small errors into some measurements.

This work was done by Andrew P. Bonifas and Luz M. Calle of **Kennedy Space Center** *and Paul E. Hintze funded by the National Research Council at Kennedy Space Center. Further information is contained in a TSP (see page 1).*

KSC-12765

Theodolite Ring Lights

These lights facilitate the use of spherical tooling balls as position references.

Goddard Space Flight Center, Greenbelt, Maryland

Theodolite ring lights have been invented to ease a difficulty encountered in the well-established optical-metrology practice of using highly reflective spherical tooling balls as position references. As described in more detail below, a theodolite ring light is attached to a theodolite or telescope and used to generate a visible target on a tooling ball.

A common technique for aiming an instrument (specifically, a theodolite or an alignment telescope) precisely at the center of a tooling ball involves the use of an autocollimating device. This technique is less than ideal because the reflection from the ball is demagnified by the spherical surface of the ball. The demagnification makes it extremely difficult to resolve the reflection and align it accurately within the cross hairs of the

The **Prototype Theodolite Ring Light** is shown here mounted on the objective-lens housing of a theodolite.

instrument. This difficulty increases with increasing distance and with decreasing size of the ball. Also, the autocollimating device adds greatly to the cost of the instrument.

A theodolite ring light produces a more easily visible reflection and eliminates the need for an autocollimating device. A theodolite ring light is a very bright light source that is well centered on the optical axis of the instrument. It can be fabricated, easily and inexpensively, for use on a theodolite or telescope of any diameter. It can be quickly mounted on or removed from the instrument. No calibration or modification of the instrument is needed. Moreover, the theodolite ring light does not reduce the field of view of the instrument and does not scatter light into the objective-lens housing of the instrument.

A theodolite ring light consists of a number of light-emitting diodes (LEDs) placed at equal angular intervals in a ring sized to fit snugly over the objective lens of the instrument. The prototype theodolite ring light, shown in the figure, includes eight 5.5-candela blue light-emitting diodes (LEDs) mounted in a ring fabricated of black polyacetal. The LEDs are powered by two D-size alkaline cells. In general, the number, brightness, and color of the LEDs can be chosen according to the conditions prevailing in a given measurement environment.

The prototype has been used to locate tooling balls of 0.5-in. (1.27-cm) and 1-in. (2.54-cm) diameter at distances from 10 to 25 ft (about 3 to 7.6 m). Operators consistently achieved accuracy and repeatability at or near the limiting resolution of the instrument. These results were significantly better than those typically obtained with conventional targets. In addition, the extreme demagnification by the small spherical target surfaces eliminated the need for calibration and for fabricating the ring to close tolerances.

This work was done by David Clark of **Goddard Space Flight Center**. *For further information, contact the Goddard Innovative Partnerships Office at (301) 286-5810.*

GSC-14898-1

Integrating Terrain Maps Into a Reactive Navigation Strategy

Traversability of terrain is taken into account as an integral part of navigation.

NASA's Jet Propulsion Laboratory, Pasadena, California

An improved method of processing information for autonomous navigation of a robotic vehicle across rough terrain involves the integration of terrain maps into a reactive navigation strategy. Somewhat more precisely, the method involves the incorporation, into navigation logic, of data equivalent to regional traversability maps. The terrain characteristic is mapped using a fuzzy-logic representation of the difficulty of traversing the terrain. The method is robust in that it integrates a global path-planning strategy with sensor-based regional and local navigation strategies to ensure a high probability of success in reaching a destination and avoiding obstacles along the way. The sensor-based strategies use cameras aboard the vehicle to observe the regional terrain, defined as the area of the terrain that covers the immediate vicinity near the vehicle to a specified distance a few meters away. The method at an earlier stage of development was described in "Navigating a Mobile Robot Across Terrain Using Fuzzy Logic" (NPO-21199), *NASA Tech Briefs*, Vol. 27, No. 2 (February 2003), page 5a. A recent update on the terrain classification stage of the method was reported in "Quantifying Traversability of Terrain for a Mobile Robot" (NPO-30744), *NASA Tech Briefs*, Vol. 29, No. 7 (July 2005), page 56. To recapitulate: The basic building blocks of the method are three behaviors that focus on successively smaller spatial scales and are integrated (in the sense of blended) through gains or weighting factors to generate speed and steering commands. The weighting factors are generated by fuzzy logic rules that take account of the current status of the vehicle.

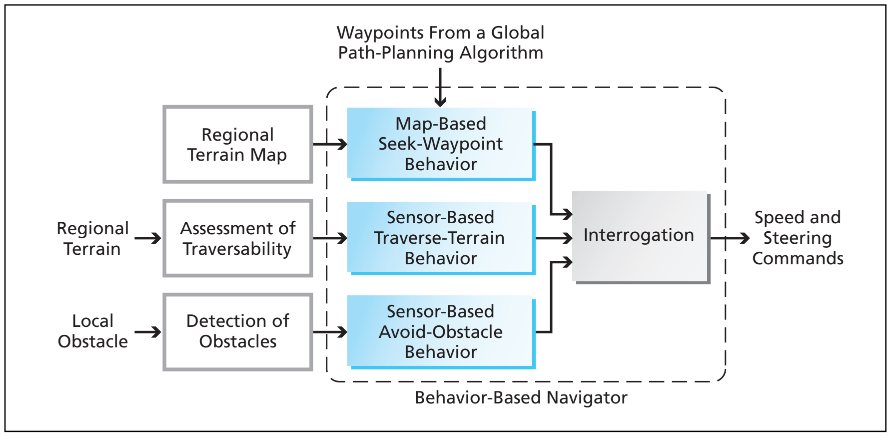

The **Navigation-System Architecture** implements three behaviors that focus on successively smaller spatial scales. These behaviors are integrated to enable safe traversal of rough terrain from a starting point to a destination.

At the present state of development, the three behaviors are denoted as a map-based seek-waypoint behavior, a sensor-based traverse-terrain behavior, and a sensor-based avoid-obstacle behavior (see figure). Navigation is initiated by a global path-planning algorithm, which generates a sequence of waypoints that define an optimal path that passes through safe (that is, sufficiently traversable) regions of the terrain from a starting point to a destination. The waypoints are fed to the map-based seek-waypoint behavior, which, as its name suggests, seeks to direct the vehicle safely from the starting location to a waypoint. The sensor-based traverse-terrain behavior determines the safest regional segment to traverse on the basis of information from regional terrain images acquired by the cameras. The sensor-based avoid-obstacle behavior involves the use of local-obstacle information from the images to develop steering and speed commands to maneuver the vehicle around the obstacles.

This work was done by Ayanna Howard, Barry Werger, and Homayoun Seraji of Caltech for **NASA's Jet Propulsion Laboratory**. *Further information is contained in a TSP (see page 1).*
NPO-30794

Reducing Centroid Error Through Model-Based Noise Reduction

Corrections are made for bias and noise.

NASA's Jet Propulsion Laboratory, Pasadena, California

A method of processing the digitized output of a charge-coupled device (CCD) image detector has been devised to enable reduction of the error in computed centroid of the image of a point source of light. The method involves model-based estimation of, and correction for, the contributions of bias and noise to the image data. The method could be used to advantage in any of a variety of applications in which there are requirements for measuring precise locations of, and/or precisely aiming optical instruments toward, point light sources.

The principal sources of centroid error are bias and noise in the outputs from the pixels of the CCD. Noise consists mainly of fixed components (readout noise and noise from dark current) and variable components (pixel defects and shot noise from background light).

Bias is caused mainly by stray light and nonuniform distribution of light in a background image.

In the present method, prior to normal operations of the CCD, one measures the point-spread function (PSF) of the telescope or other optical system used to project images on the CCD. The PSF is used to construct a database of spot models representing the nominal CCD pixel outputs for a point light source projected onto the CCD at various positions incremented by small fractions of a pixel (see figure).

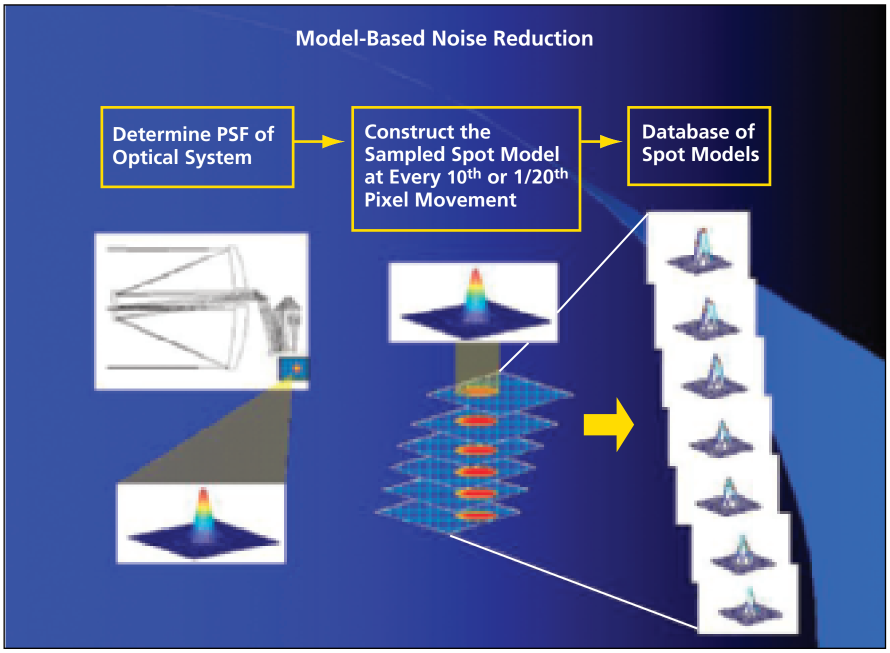

Spot Models are constructed from the measured PSF. The spot models are thereafter used in processing digitized CCD outputs to correct for bias and noise to refine centroid estimates.

During normal operation of the CCD, the centroid of the image of a point source of light is initially computed from the digitized CCD pixel outputs in the conventional way. However, this initial computation of the centroid is used to retrieve the corresponding spot model that was constructed earlier. Then the boundary between noise and signal is determined by comparing the spot model with the CCD pixel outputs. Pixel positions of same pixel value of the spot model and the image data in the background area are defined as the boundary. All pixels of the image data beyond this boundary are set to zero. This effectively removes the noise and bias in the subsequent centroid estimation from the corrected image data.

This work was done by Shinhak Lee of Caltech for **NASA's Jet Propulsion Laboratory**. *Further information is contained in a TSP (see page 1).*

NPO-30585

Adaptive Modeling Language and Its Derivatives

Modeling language enables automation of the entire product development cycle.

TechnoSoft, Inc., Cincinnati, Ohio

Adaptive Modeling Language (AML), developed by TechnoSoft, Inc., is the underlying language of an object-oriented, multidisciplinary, knowledge-based engineering framework. TechnoSoft is a leading provider of object-oriented modeling and simulation technology used for commercial and defense applications. AML offers an advanced modeling paradigm with an open architecture, enabling the automation of the entire product development cycle, integrating product configuration, design, analysis, visualization, production planning, inspection, and cost estimation.

The AML framework is truly adaptive. Its successful history includes a wide variety of defense and commercial applications including aerospace, automotive, and capital equipment.

TechnoSoft has worked with the Vehicle Analysis Branch (VAB) at NASA LaRC on the development of the Collaborative Hypersonic Airbreathing Vehicle Environment (CoHAVE) built using AML. The collaborative enterprise environment of CoHAVE and its criteria-management environment are applicable to the design of NASA, military, and private commercial vehicles.

CoHAVE is applicable to the Reusable Space Transportation System's product area for evaluating the architectures of the Space Transportation Architecture Studies and Second Generation RLV Studies. Elements of this architecture include enhanced Shuttle, Reusable Two Stage to Orbit, and Venture Star (an SSTO design). Complementary to these delivery vehicles are Orbital Transfer Vehicles, Crew Transfer and Crew-Cargo Transfer Vehicles, and the Reusable First Stage Booster for Space Shuttle Upgrades. CoHAVE is platform independent and enables multiple users to collaborate across geographically-distributed, heterogeneous workstations. CoHAVE provides a comprehensive environment that facilitates the performance of concurrent engineering of hypersonic airbreathing vehicles at a level not currently available.

Recently, CoHAVE has been extended to incorporate models for other applications such as re-entry vehicles. Since the environment now includes vehicles other than traditional hypersonic airbreathing vehicles, the name has morphed into the Advanced Vehicle Integration and Synthesis Environment (AdVISE).

This work was done by Adel Chemaly of **TechnoSoft, Inc.** *under a NASA Small Business Innovation Research (SBIR) contract monitored by* **Langley Research Center**. *For further information, contact:*

Mr. Adel Chemaly
TechnoSoft, Inc.
11180 Reed Hartman Hwy.
Cincinnati, OH 45242
Phone No.: (513) 985-9877
E-mail: adel.chemaly@technosoft.com
Web site: www.technosoft.com.

Refer to SBIR-0012, volume and number of this NASA Tech Briefs *issue, and the page number.*

Books & Reports

Stable Satellite Orbits for Global Coverage of the Moon

A document proposes a constellation of spacecraft to be placed in orbit around the Moon to provide navigation and communication services with global coverage required for exploration of the Moon. There would be six spacecraft in inclined elliptical orbits: three in each of two orthogonal orbital planes, suggestive of a linked-chain configuration. The orbits have been chosen to (1) provide 99.999-percent global coverage for ten years and (2) to be stable under perturbation by Earth gravitation and solar-radiation pressure, so that no deterministic firing of thrusters would be needed to maintain the orbits. However, a minor amount of orbit control might be needed to correct for such unmodeled effects as outgassing of the spacecraft.

This work was done by Todd Ely of Caltech and Erica Lieb of ASRC for **NASA's Jet Propulsion Laboratory**. *Further information is contained in a TSP (see page 1). NPO-42722*

Low-Cost Propellant Launch From a Tethered Balloon

A document presents a concept for relatively inexpensive delivery of propellant to a large fuel depot in low orbit around the Earth, for use in rockets destined for higher orbits, the Moon, and for remote planets. The propellant is expected to be at least 85 percent of the mass needed in low Earth orbit to support the NASA Exploration Vision. The concept calls for the use of many small (≈10 ton) spin-stabilized, multistage, solid-fuel rockets to each deliver ≈250 kg of propellant. Each rocket would be winched up to a balloon tethered above most of the atmospheric mass (optimal altitude 26 ±2 km). There, the rocket would be aimed slightly above the horizon, spun, dropped, and fired at a time chosen so that the rocket would arrive in orbit near the depot. Small thrusters on the payload (powered, for example, by boil-off gasses from cryogenic propellants that make up the payload) would precess the spinning rocket, using data from a low-cost inertial sensor to correct for small aerodynamic and solid rocket nozzle misalignment torques on the spinning rocket; would manage the angle of attack and the final orbit insertion burn; and would be fired on command from the depot in response to observations of the trajectory of the payload so as to make small corrections to bring the payload into a rendezvous orbit and despin it for capture by the depot. The system is low-cost because the small rockets can be mass-produced using the same techniques as those to produce automobiles and low-cost munitions, and one or more can be launched from a U.S. territory on the equator (Baker or Jarvis Islands in the mid-Pacific) to the fuel depot on each orbit (every 90 minutes, e.g., any multiple of 6,000 per year).

This work was done by Brian Wilcox of Caltech for **NASA's Jet Propulsion Laboratory**. *Further information is contained in a TSP (see page 1). NPO-42007*

National Aeronautics and
Space Administration